Cotton-Mouton Effect Measurement in a Plasma at the W7-AS Stellarator

Ch. Fuchs and H. J. Hartfuss
Max-Planck-Institut für Plasmaphysik, EURATOM Association, D-85748 Garching, Germany
(Received 23 December 1997)

A Cotton-Mouton effect polarimeter operating in the submillimeter wave region has been developed at the W7-AS stellarator. The transmission matrix representative for the change of polarization state of a probing wave has been calculated and significant elements are determined experimentally. Systematic magnetic field scans over a wide range of the magnetic field conducted at two different probing frequencies were carried out for the first time. These scans clearly demonstrate that the Cotton-Mouton effect is being observed under optimal experimental conditions. The experimental setup measures the line integrated electron density unambiguously and has proven its robustness under various conditions. [S0031-9007(98)06945-2]

PACS numbers: 52.70.Gw, 52.55.Hc

Recent interest in the Cotton-Mouton effect in fusion relevant plasmas arises from the quest for a robust measurement of the line integrated electron density for control purposes in future long pulse machines as proposed for ITER [1]. The effect was first discovered in liquids [2] and is widely used in fundamental research in various fields [3].

A magnetized plasma is linear and circular birefringent. Both properties can be used for diagnostic purposes. Under ideal conditions with an electromagnetic wave propagation perpendicular or parallel to the magnetic field, the effects can be separated giving rise to a change in ellipticity of a wave owing to the Cotton-Mouton effect or a rotation of its plane of polarization owing to the Faraday effect, respectively.

The Cotton-Mouton effect has been discussed by de Marco and Segre [4] and in numerous papers by Segre [5,6], and references therein, from a fundamental point of view as well as for diagnostic applications. In earlier experiments the effect has been measured by Shevchenko *et al.* [7] and Grolli and Maddaluno [8]. More detailed studies have been conducted at the W7-AS stellarator with emphasis both on elucidating the Cotton-Mouton part within Segre's formalism and demonstrating its diagnostic capabilities.

The net current free W7-AS stellarator offers optimal conditions for this purpose by providing lines of sight with $|B| \simeq \text{const}$ and $B_{\parallel} = 0$. The B field is negligibly affected by internal plasma diamagnetism and local pressure driven currents. The basic principles of the measurements are discussed in terms of the general formalism and results for various conditions particularly for different B fields and probing beam frequencies are given.

Basics and results of the measurement.—The basis of the measurement is the change of the polarization of an electromagnetic wave passing a magnetized plasma. Following the formalism in the literature [5,6], the state of polarization can be described by the Stokes vector $\vec{s}(z)$ with components $s_1(z)$, $s_2(z)$, and $s_3(z)$. The evolution along the line of sight (z direction) is given by

$$\frac{d\vec{s}(z)}{dz} = \vec{\Omega}(z) \times \vec{s}(z) . \tag{1}$$

The vector $\vec{\Omega}(z)$ describes the plasma wave interaction. For $\omega^2 \gg \omega_p^2$ and $\omega^2 \gg \omega_c^2$, where ω_p and ω_c are the plasma and the electron cyclotron angular frequencies and $\omega = 2\pi f$, the approximation

$$\begin{pmatrix} \Omega_1 \\ \Omega_2 \\ \Omega_3 \end{pmatrix} = \frac{\omega_p^2}{2c\omega^3} \begin{pmatrix} \frac{e^2}{m^2}(B_x^2 - B_y^2) \\ \frac{e^2}{m^2} 2B_x B_y \\ 2\omega \frac{e}{m} B_z \end{pmatrix} \tag{2}$$

can be made. The components Ω_1 and Ω_2 represent the Cotton-Mouton, while Ω_3 describes the Faraday effect. If the magnetic field vector $\vec{B}$ is parallel to the x or y axis of the chosen coordinate system then $\Omega_2 = 0$. Exact expressions for the components of $\vec{\Omega}$ are given in [5]. An example of n_e, $\vec{B}$, and the components of $\vec{\Omega}$ along the chosen line of sight in W7-AS is shown in Fig. 1.

The Stokes vector $\vec{s}$ is a unit vector which changes only its direction in a birefringent medium; $\vec{\Omega}$ then defines the rotation axis. The birefringent properties of the medium

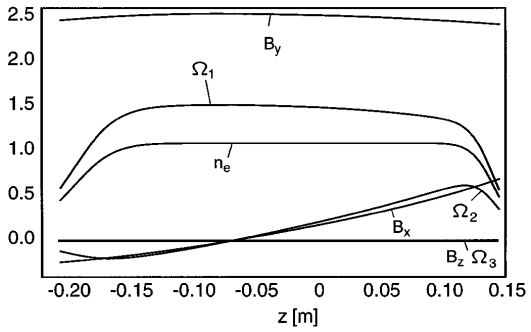

FIG. 1. The magnetic field B (in T), the electron density n_e (in 10^{20} m^{-3}) and Ω_1, Ω_2, and Ω_3 (in -0.5 rad/m) for a typical plasma at the W7-AS stellarator along the line of sight chosen for this experiment.

 0031-9007/98/81(8)/1626(4)$15.00

can therefore be described by a matrix **M** connecting the polarization states $\vec{s}(z_0)$ and $\vec{s}(z_1)$ when entering and leaving the plasma, respectively:

$$\vec{s}(z_1) = \mathbf{M}(z_1) \cdot \vec{s}(z_0). \tag{3}$$

For $|W_i| \ll 1$ with $W_i(z_1) = \int_{z_0}^{z_1} dz\, \Omega_i(z)$, the matrix **M** can be approximated analytically [6]. The diagonal elements are 1 and all other elements are composed of two parts: a first order component W_i as defined before and a second order one $W_{ik} = \int_{z_0}^{z_1} dz\, \Omega_i(z) \int_{z_0}^{z} dz'\, \Omega_k(z')$. Segre proposed different modulation schemes which allow for the determination of the elements of the transmission matrix **M** [6]. However, extremely high phase measurement accuracy is demanded in this case. For the line of sight at W7-AS all matrix elements which do not include the component W_1 are too small to be measured owing to the experimental uncertainties involved. In order to keep errors low, the measurements were conducted at high electron densities n_e resulting in W_1 close to 1 for probing beam frequencies in the range 500–650 GHz. In this case the analytic approximation as given in [6] is not valid.

In a similar approximation as applied in [9] under conditions where the Faraday effect is dominant, the transmission matrix for Cotton-Mouton effect dominated conditions is given by

$$\mathbf{M}(\mathbf{z}_1) = \begin{pmatrix} 1 & -P_1^{(0)} & Q_1^{(0)} \\ P_1^{(0)} \cos W_1 + Q_1^{(0)} \sin W_1 & \cos W_1 & -\sin W_1 \\ P_1^{(0)} \sin W_1 - Q_1^{(0)} \cos W_1 & \sin W_1 & \cos W_1 \end{pmatrix} \tag{4}$$

with

$$W_1(z) = \int_{z_0}^{z} dz'\, \Omega_1(z'), \qquad W_1 = W_1(z_1)$$

and

$$P_1^{(0)} = \int_{z_0}^{z_1} dz[\Omega_3(z) \cos W_1(z) - \Omega_2(z) \sin W_1(z)],$$

$$Q_1^{(0)} = \int_{z_0}^{z_1} dz[\Omega_3(z) \sin W_1(z) + \Omega_2(z) \cos W_1(z)].$$

The quantity W_1 is in lowest order the phase shift between the x- and y-polarized components owing to the Cotton-Mouton effect with B mainly in the y direction. Full numerical calculations of **M** for the experimental conditions at W7-AS show that even for the maximum tolerance of the line of sight considered $|W_3| \leq 0.2|W_1|$ and $|W_2| \leq 0.1|W_1|$. Although the condition $\Omega_1 \gg \Omega_2$ is not fulfilled at the edge of the plasma (Fig. 1), all matrix elements as calculated with Eq. (4) show no significant difference to full numerical results for $n_e = 1.5 \times 10^{20}\ \mathrm{m}^{-3}$; the absolute values of M_{12}, M_{13}, M_{21}, and M_{31} are maximally $0.2|W_1|$. All matrix elements are functions of W_1 and the quantities $P_1^{(0)}$ and $Q_1^{(0)}$. Again, they can be determined experimentally by applying the various modulation techniques as proposed in [6]. However, under the chosen experimental conditions, the elements M_{12}, M_{13}, M_{21}, and M_{31} are again too small to be determined; systematic errors would have to be within 1^0 in phase for such measurements. The elements M_{22}, M_{23}, M_{32}, and M_{33} in contrast can easily be determined with sufficient accuracy by measuring W_1.

To achieve this, the phase difference between the x- and the y-polarized components (with equal amplitudes) of the probing wave is modulated with frequency ω_m. The resulting components of the Stokes vector $\vec{s}(z_0)$ are $s_1(z_0) = 0$, $s_2(z_0) = \cos(\omega_m t)$, and $s_3(z_0) = \sin(\omega_m t)$. Using Eq. (4) the polarization state of the probing wave leaving the plasma can be determined. Particularly the Stokes parameter $s_2(z_1)$ is given by $s_2(z_1) = \cos(\omega_m t + W_1)$, which shows that W_1 can simply be measured as a phase difference in s_2 before and after the plasma transmission. The component s_2 is measured with a linear analyzer rotated by 45° with respect to the x axis.

To compare theory and experiment and to give an example for the transmission matrix **M**, a real plasma discharge with a central electron density $n_e = 0.78 \times 10^{20}\ \mathrm{m}^{-3}$ is used; density data are taken from the multichannel interferometer and Thomson scattering diagnostics. The magnetic field is $B = 2.5$ T, the edge rotational transform is 0.36, and the probing beam frequency is 535 GHz. The transmission matrix calculated from these data is

$$\mathbf{M}(\mathbf{z}_1) = \begin{pmatrix} 1.00 & 0.04 & -0.05 \\ 0.00 & 0.81 & 0.59 \\ 0.06 & -0.59 & 0.81 \end{pmatrix}. \tag{5}$$

The measured value for W_1 under these conditions is $W_{1_m} = -0.65$ and compares well with the calculated value of -0.63 so that also $\cos W_{1_m} = 0.79$ and $\sin W_{1_m} = -0.61$ show good agreement with the calculated elements M_{33} and M_{32}.

The line integrated density $\rho_e = \int_{z_0}^{z_1} n_e\, dz$ is derived from W_1 in the following way. The $B \simeq$ const condition allows for a separation of ρ_e and the B-dependent part of W_1. Taking the exact expression for Ω_1, as given in [5], W_1 is not exactly proportional to ρ_e. The exact expression $\Omega_{1_{\mathrm{ex}}}$ can be written as the product of the high frequency approximation $\Omega_{1_{\mathrm{app}}}$ and a factor k which corrects for higher order terms in n_e and B. Introducing the linearized phase shift per unit line density G, the following equation is obtained:

$$|W_1| = G\overline{k}\rho_e. \tag{6}$$

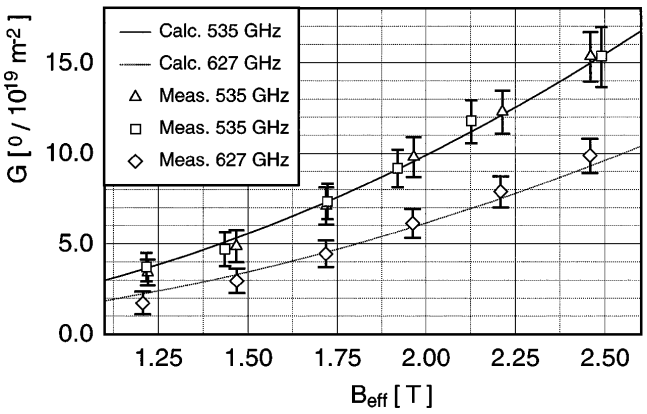

FIG. 2. Measurements of the phase shift per line density, G, for two frequencies and different magnetic fields compared to calculated curves for G. The measurements were conducted at $n_e \approx 1 \times 10^{20}$ m^{-3}.

The quantity G is calculated using the high frequency approximation for Ω_1 as $G = |\int_{z_0}^{z_1} dz\, \Omega_1(z)/n_e(z)|$. Introducing the effective magnetic field,

$$B_{\text{eff}}^2 = \left| \int_{z_0}^{z_1} f_{\text{prof}}(B_x^2 - B_y^2)\, dz \right| \Big/ \int_{z_0}^{z_1} f_{\text{prof}}\, dz\,, \quad (7)$$

where f_{prof} is a trapezoid profile function for the electron density n_e with n_e rising within 20% of the length of the sightline; G turns out to be

$$G = (6.62 \times 10^{-13}\ \text{m}^2) f^{-3} B_{\text{eff}}^2\,, \quad (8)$$

where f is in GHz and B_{eff} in Tesla. The factor $\overline{k}$ which is typically <1.1 is the mean value of $k = \Omega_{1_{\text{ex}}}/\Omega_{1_{\text{app}}}$. An approximate expression for $\overline{k}$ can easily be derived:

$$\overline{k} = 1 + f^{-2}(784B^2 + 12\,092\overline{n_e}) \quad (9)$$

with f and B in the same units as before and $\overline{n_e}$ in 10^{20} m^{-3}. The quantity $\overline{k}$ is linear in the mean electron density $\overline{n_e}$ as easily derived from ρ_e. In this way, Eq. (6) contains ρ_e up to the second order which allows for a simple but almost correct calculation of ρ_e. The quantity $G = |W_1|/(\overline{k}\rho_e)$ is exactly proportional to $f^{-3}B_{\text{eff}}^2$. By verifying the f and B_{eff} dependencies of G, derived from measured values of W_1, it can be shown that the Faraday effect with its different parameter dependency, $\Omega_{3_{\text{app}}} \propto Bf^{-2}$, is of negligible concern. Therefore the matrix elements M_{22}, M_{23}, M_{32}, and M_{33} can be calculated using Eq. (4) from the measured phase W_1.

Measurements of W_1 are conducted at magnetic fields in the range $B_{\text{eff}} = 1.2$–2.5 T and at two frequencies, 535 and 627 GHz. The scans are conducted at fixed frequency, scanning the field on a shot-to-shot basis. In order to rely on absolute values of G, the line density as measured with the interferometer is used for evaluation. The results are presented in Fig. 2. All measured values agree with those calculated within error bars. Experimental errors will be discussed below.

Experimental setup.—The total experimental setup is sketched in Fig. 3. A backwardwave oscillator (BWO) is used as a tunable radiation source in the frequency range 500—650 GHz. Oversized waveguides ($\phi = 24$ mm) are used throughout in the guided wave sections. The modulation of the wave ellipticity is accomplished in a way as described in [7]. A polarizing wire grid reflects the y-polarized component of the wave, whereas the x component is guided to a delay line. After reflection at

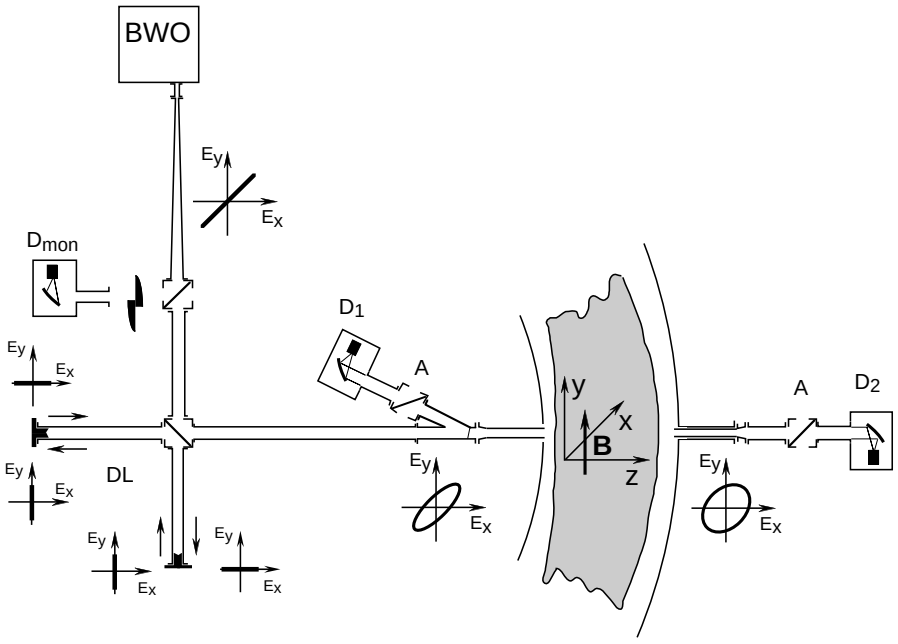

FIG. 3. Experimental setup at the W7-AS stellarator. The E_y-E_x diagrams illustrate the state of polarization and refer to the coordinate system given at the location of the plasma.

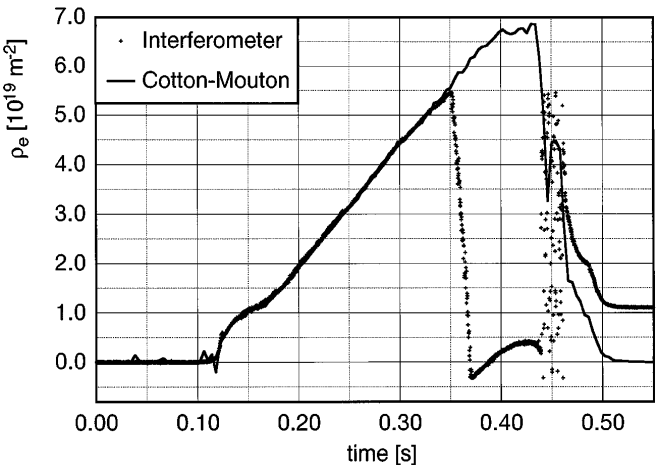

FIG. 4. Line densities measured by the Cotton-Mouton polarimeter at $f = 535$ GHz and the microwave interferometer at $f = 160$ GHz. For this experiment B is 2.5 T.

two mirrors which rotate the polarization plane by 90° this component is added to the reflected one. The phase difference of the two components depends on the wave frequency and the length of the delay line. A BWO-frequency modulation with $\Delta f = 300$ MHz then transforms to an ellipticity modulation of the probing wave. Detectors D_1 and D_2 with 45° analyzers (A) act as reference and signal detectors delivering signals proportional to $s_2(z_0)$ and $s_2(z_1)$, respectively. Their phase difference is the quantity of interest which is evaluated digitally. Errors introduced by unwanted amplitude modulation of the BWO are eliminated by the interpretation code with data from the detector D_{mon} which is monitoring the BWO output power.

The largest error contribution comes from the properties of the transmission line. Small changes of the polarization cause errors in the W_1 measurement of about 1%. Considering also misalignments in the probing beam path, numerical calculations result in maximum errors between -3% and $+2\%$ for the lowest B field (1.25 T) where the effect is smallest. Another error results from different phase shifts for the x and y components in the transmission line in combination with BWO instabilities which lead to phase errors of about 1%. Other errors include amplitude modulation caused by the frequency dependent vacuum window transmission, plasma diamagnetism, and uncertainities in the probing beam frequency. Errors owing to refraction effects, which could lead to a path length difference for the x- and the y-polarized components of the probing beam, are negligible as proven by ray tracing calculations. The relative errors sum up to an error range of -5.5% to 5.6% for $B = 1.25$ T and -4.5% to 5.1% for $B = 2.5$ T in maximum, including maximum misalignment of the probing beam.

Line density measurements.—The results from the Cotton-Mouton polarimeter have been compared in many discharges with those obtained with the multichannel interferometer installed at W7-AS. One example with a central electron density of up to 2×10^{20} m^{-3} is given in Fig. 4. Evaluation is done on the basis of Eq. (6) as described before. Good agreement is obtained in all measurements. The resolution $\Delta\rho_e$ of a line density measurement for the Cotton-Mouton polarimeter is dependent on B_{eff}, f, and the signal-to-noise ratio. The phase resolution is 0.2° for 1 ms of time resolution. For the same signal-to-noise ratio, $\Delta\rho_e$ is worse compared with typical interferometers because of the lower phase differences involved. However, the stability and robustness is much higher because no reference beam is needed and phase differences remain below 360° so that keeping track of fringe jumps is not necessary. The robustness and absolute measurement capability was demonstrated by switching the probing beam on and off during a discharge. The polarimeter was able to resolve the temporal density increase during pellet injection with a 100 μs time resolution. It has also been used for density control of the machine.

In conclusion, the experimental efforts in the course of the studies presented show that it is experimentally very difficult to determine the elements of the transmission matrix for an arbitrary sightline under the condition $|W_i| \ll 1$. For a sightline chosen where the Faraday effect is negligible the elements containing W_1 could be measured with good accuracy. By measuring the frequency and magnetic field dependencies the assumption that the Faraday effect is negligible could be verified.

The capability of the Cotton-Mouton effect for a robust measurement of the line integrated density at W7-AS has been demonstrated. It offers a great advantage for long pulse machines like the future W7-X. Both W7-X and W7-AS offer a favorable magnetic field topology for the method.

The main problems of the W7-AS setup are the transmission properties of the oversized waveguides with respect to conservation of the polarization state. This could possibly be avoided by using quasioptical transmission if space allows. An absolute phase resolution of 0.1° might be possible for a setup optimized in this way.

The authors thank Professor S. E. Segre and Dr. P. Buratti for their proposals and helpful discussions.

[1] P. Buratti, proposed and discussed at meetings with the European Home Team on microwave diagnostics for ITER, 1995 (unpublished).
[2] A. Cotton and H. Mouton, C. R. Acad. Sci. **141**, 317 (1905); **141**, 349 (1905).
[3] G. Maret, in *Physical Phenomena at High Magnetic Fields*, edited by E. Manousakis (Addison-Wesley, Redwood City, 1992), p. 459.
[4] F. de Marco and S. E. Segre, Plasma Phys. **14**, 2452 (1972).
[5] S. E. Segre, Plasma Phys. **20**, 295 (1978).
[6] S. E. Segre, Phys. Plasmas **2**, 2908 (1995).
[7] V. F. Shevchenko, A. A. Petrov, V. G. Petrov, and Y. A. Chaplygin, Plasma Phys. Rep. **22**, 28 (1996).
[8] M. Grolli and G. Maddaluno, Nucl. Fusion **22**, 961 (1982).
[9] S. E. Segre, Phys. Plasmas **3**, 1182 (1996).